Remote Sens. **2014**, *6*, 8220-8237; doi:10.3390/rs6098220

OPEN ACCESS

remote sensing

ISSN 2072-4292

www.mdpi.com/journal/remotesensing

Article

Assessment of Complex Masonry Structures with GPR Compared to Other Non-Destructive Testing Studies

Sonia Santos-Assunçao [1], Vega Perez-Gracia [1,*], Oriol Caselles [2], Jaume Clapes [2] and Victor Salinas [2]

[1] Department of Strength of Materials and Structural Engineering, Escola Universitària d'Enginyeria Tècnica Industrial, Technical University of Catalonia, C/Urgell 187, 08036 Barcelona, Spain; E-Mail: sonia.assuncao@upc.edu

[2] Department of Geotechnical Engineering and Geo-Sciences, Technical University of Catalonia, C/Jordi Girona 1-3, 08034 Barcelona, Spain; E-Mails: oriol.caselles@upc.edu (O.C.); victor.salinas@upc.edu (J.C.); victor.salinas@upc.edu (V.S.)

* Author to whom correspondence should be addressed; E-Mail: vega.perez@upc.edu; Tel.: +34-934-137-333; Fax: +34-934-137-431.

Received: 20 June 2014; in revised form: 21 August 2014 / Accepted: 25 August 2014 / Published: 29 August 2014

Abstract: Columns are one of the most usual supporting structures in a large number of cultural heritage buildings. However, it is difficult to obtain accurate information about their inner structure. Non-destructive testing (NDT) methodologies are usually applied, but results depend on the complexity of the column. Non-flat external surfaces and unknown and irregular internal materials complicate the interpretation of data. This work presents the study of one column by using ground-penetrating radar (GPR) combined with seismic tomography, under laboratory conditions, in order to obtain the maximum information about the structure. This column belongs to a "Modernista" building from Barcelona (Spain). These columns are built with irregular and fragmented clay bricks and mortar. The internal irregular and complex structure causes complicated 2D images, evidencing the existence of many different targets. However, 3D images provide valuable information about the presence and the state of an internal tube and show, in addition, that the column is made of uneven and broken bricks. GPR images present high correlation with seismic data and endoscopy observation carried out *in situ*. In conclusion, the final result of the study provides information and 3D images of damaged areas and inner structures. Comparing the different methods to the real structure of the column, the potential and limitations of GPR were evaluated.

Keywords: ground-penetrating radar (GPR); seismic tomography; cultural heritage; masonry column; cylindrical interpolation; 3D radar imaging

1. Introduction

All building materials and structural members deteriorate with age and exposure to the weather. However, in most cases, damages cannot be detected by visual inspection. Hence, the application of non-destructive testing methodologies could be a helpful assessment in structural evaluations and further restorations, their information being crucial in the structural evaluation. Ancient buildings and cultural heritage buildings require particular surveillance in structural assessment, because of the small amount of knowledge of the inner geometry, constructive materials and state of conservation. Understanding the interior of the structures is the first stage to evaluate their state and to design potential repairs. However, the special character of historical and cultural heritage buildings makes the integral inspection difficult, as some methodologies are invasive and deteriorate or affect the structure. Therefore, non-destructive testing (NDT) techniques are commonly used prior to inspection, while other invasive techniques are applied only in doubtful and more complex areas. The result of the inspection tasks must provide the most realistic description of the state of the building and the inner structure. There is a great variety of possible classes of defects in buildings, involving different parts of the structure. A comprehensive description of several building pathologies and the most useful testing methodologies can be found in [1]. In the case of cultural heritage, geophysical surveys are some of the methodologies commonly applied in structural assessment. Several examples can be found in the literature, based on different survey systems (e.g., [2–6]). Two main limitations exist in the application of these surveys: they are indirect measurements, and the space available for surveys in many parts of the historical buildings is limited. As a consequence of the first limitation, the results do not have a single valid interpretation. Then, uncertainty appears in all conclusions, and results must be compared to previous knowledge or to results from other inspections. Regarding the second limitation, some geophysical exploration requires extensive and flat areas, without obstacles. In some cases, reduced areas limit the penetration depth and, in other cases, make impossible the application of these technologies.

Ground penetrating radar (GPR) is one of the most significant geophysical techniques applied in building inspection (e.g., [4,7,8]), as a consequence of its high resolution [9,10] and applicability in typical structural members. Its portability in terms of weight and size makes access to different zones easier. However, this method detects changes in electromagnetic properties, and mechanical parameters from constructive materials cannot be inferred from GPR records. A combination of GPR inspection with seismic evaluation could offer more informative interpretations and help in the accurate analysis of the possible uncertainties. The applicability of seismic surveys in cultural heritage buildings has been proven as a successful tool in diverse works (e.g., [3,5]). The main difficulty of GPR or combined surveys lies in the existence of complex structures. Complexity could be a consequence of non-flat surfaces. Therefore, applicability and interpretation could be arduous or even impossible. Complexity could be also a consequence of irregular shapes and arrangements of the

internal elements: irregular brick arrangement, the existence of many different materials and objects or asymmetric and numerous targets. In all of these cases, numerous reflections and diffractions are produced in all of the irregular targets, and data appear confused, making the interpretation difficult. Combining methodologies is a strategy used to corroborate results (e.g., [11]) and to obtain accurate interpretations.

Different strategies have been used in order to improve interpretations and results. For example, simulation and laboratory tests in simple and flat masonry samples have been carried out with the purpose of enhancing the GPR processing data for the detection of unfilled joints [12], highlighting the difficulty in recognizing reflections caused by voids in real data, but without obtaining realistic images of the media. More complex walls were also evaluated to define irregularities by means of GPR tomography [13]. Other structures, such as masonry arch bridges, were also tested in laboratory and simulated in order to define the crack size range that could be detected with GPR [14] and evaluated in different applications [15,16]. Although applications in flat walls of cultural heritage buildings have been increasing, obtaining good results (e.g., [17]), the study of columns is still a complicated issue because of the geometry of the structures, which is, in many cases, cylindrical. A discussion about the effects of the cylindrical geometry on the radar data was developed by [18], applied to homogeneous columns. Good examples of applications in cylindrical columns made of stone, obtaining circular radargrams, can be found in [19]. This notwithstanding, a large number of cultural heritage buildings are masonry structures constructed with small bricks, which have not been extensively studied yet.

In this work, several tests were performed in one masonry column under laboratory conditions. Externally, the member seems to be built with small bricks, but its internal structure is unknown. This column is found as a supporting structure in Art Noveau ("Modernista") buildings in Barcelona. This complex of buildings is part of the "Modernista" cultural heritage of the city. Non-destructive tests were carried out in the column. Ground penetrating radar was used in order to obtain three-dimensional images of the inner column, and seismic tomography was applied in order to define the properties of the internal elements and to obtain two-dimensional sections that allowed us to corroborate some GPR results. Those NDT studies were complemented with endoscopy and with a final destructive evaluation that provide direct information about the internal shape and elements. The adequacy of the geophysical NDT surveys was evaluated by comparing the direct images of the inner column to the radar and seismic images.

2. Objectives and Methodology

The Hospital of Sant Pau i la Santa Creu is considered one of the most important "Modernista" monuments in Barcelona. This huge complex was designed by the architect, Lluís Domènec i Muntaner, in 1905, and it is composed of numerous buildings communicated by underground tunnels. The buildings are supported by masonry columns. During the last few years, several intensive restoration tasks were performed as a consequence of the failure of one dome. The evaluation paid attention to the columns, which appear deteriorated in many parts of the complex. Fissures and dampness seem to be some of the most common pathologies observed on a preliminary visual inspection of those columns. Figure 1 shows the main entrance of the complex, the interior of one of the buildings and some images of the pathologies observed in the columns. Damages caused by corrosion also appear in several of the

columns, indicating the existence of some metallic element embedded into the column. Other columns present visible humidity effects, even in the case of members in internal rooms. In several members, fissures and cracks appear on the surface, and some of the columns present ancient restorations.

Pathologies detected after the first visual inspection were numerous, and wider studies were necessary in order to evaluate the structural behavior of the building. Mechanical and chemical damages, like fissures, oxidations and loss of the outer coating of the bricks, appear in many of the columns. Furthermore, the arrangement of the bricks is unknown, as is the possible existence of metallic reinforcing rings or rain drain pipes. Hence, NDT exploration was planned by means of GPR and seismic tomography. Previously, in order to define the ability of the NDT methods, to determine the best radar data acquisition methodology and the most appropriate data processing, some tests were performed in the laboratory using one of the columns that was extracted from its original place.

Figure 1. Hospital de Sant Pau i la Santa Creu. (**a**) View of the main façade; (**b**) internal view of one pavilion; (**c**) scheme of the supporting structures in the internal pavilion; (**d**) damage in columns caused by corrosion; (**e**) fissures in masonry columns; (**f**) moisture affecting the exterior of the columns.

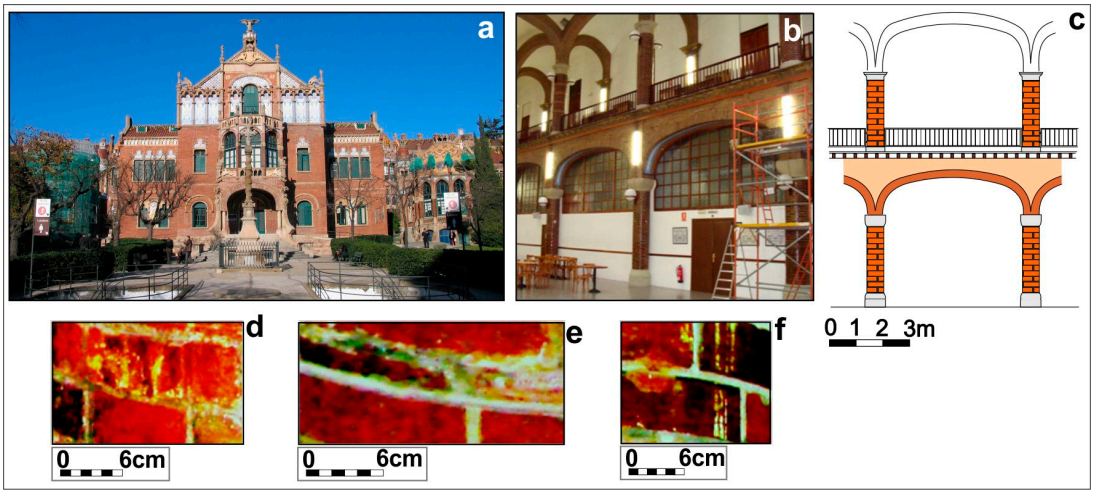

This work describes the tests performed in the laboratory and highlights the ability and possible limitations in further GPR and seismic surveys. The evaluation of the entire building could be carried out considering the results and conclusions obtained in this preliminary study.

The main objectives of the laboratory test were: obtaining horizontal radar slices and three-dimensional images, showing the different targets existing inside the column; detecting changes of seismic wave velocity inside the column; and comparing geophysical results to the images resulting from the subsequent endoscopy and after breaking the column.

The column was taken to the laboratory with a compressive jacket. Afterwards, it was placed on a sand bed. The specimen is 64 cm in diameter and 145 cm tall. The surface is covered by masonry clay bricks measuring 12 cm × 6 cm each, but with unknown variable thickness and irregular internal shape (see Figure 2). The presence of corrosion damage outside of some of the columns in the building evidences the existence of some metallic elements inside the structure. Attending to a preliminary structural estimation, these elements could be vertical reinforcements. Hence, one of the purposes of

the laboratory inspection in the sample is to corroborate or refute this assumption, defining the position and approximate size of these elements if they do exist.

Figure 2. Preparing the specimen for the test. (**a**) The column with the metallic jacket; (**b**) the test site; (**c**) the column prepared to be tested; (**d**) the distance between horizontal and vertical radar lines.

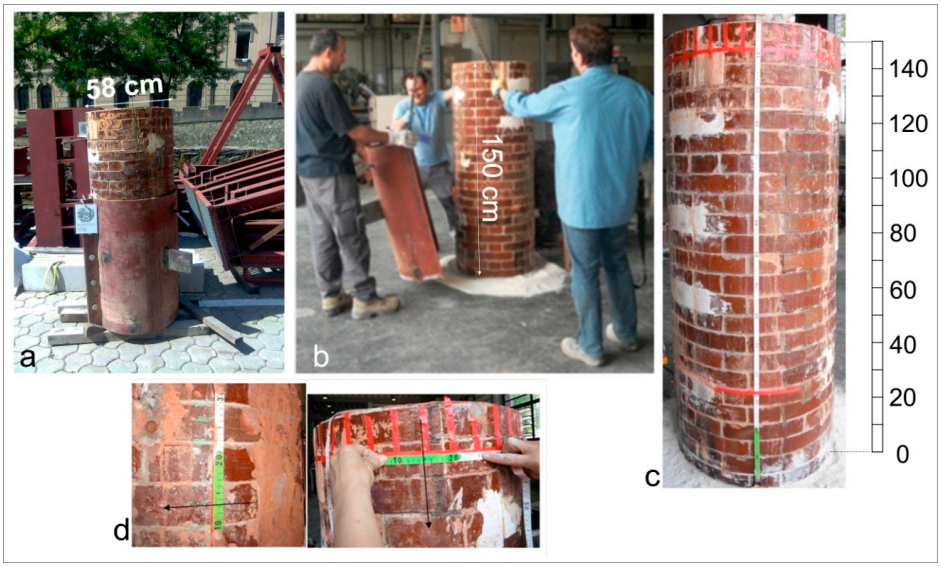

2.1. Ground-Penetrating Radar

Vertical and horizontal lines were marked on the surface, spaced 5 cm and 3 cm, respectively, in order to acquire GPR data along each one. A Ramac radar was used in the test, with a 1.6-GHz center frequency antenna. The position on the column was determined with a survey-wheel odometer. During the radar acquisition, the sampling frequency was 86,200 MHz, obtaining 672 samples per trace. The spatial sampling was 0.002 m, and the temporal window was 8 ns. Some preliminary tests seem to indicate that the average wave velocity was about 10 cm/ns. These tests were carried out with direct measurements, knowing the diameter of the column and obtaining the reflection on a metallic target placed on the opposite side of the antenna. Later and more accurate measurements, after the strength analysis, indicate that the average velocity could be higher, close to 13 cm/ns. In this case, the column was broken, showing the existence of a central metallic tube. The exact diameter of this metallic tube was measured. Reflection on this target was clearly visible in all radargrams presenting small changes in the two-way travel time. Hence, velocity was defined by comparing the mean two-way travel time to this anomaly with the distance corresponding to the radius of the column minus the radius of the internal tube.

B-scans were processed with GPRSlice software [20,21] in order to obtain 2D slices and 3D images. The sequence processing applied to each radargram was: search for time, 0 ns; subtract DC-shift; dewow and band pass filter within 500 MHz and 2200 MHz. A manual gain function (Figure 3) was also applied.

After the sequence processing, horizontal radargrams were transformed into cylindrical coordinates, covering 328° and along 110 m of the column. Radargrams were linearly interpolated, and circular

horizontal slices were obtained by the spatial average of the squared waves amplitudes. Time slices were obtained from intervals of 1.2 ns, along the 8 ns total time window. A total number of 15 intervals allow overlapping time slices, to define the continuity of reflections in consecutive images. Finally, identification of the 3D volume was possible by the isosurface rendering imaging with a cutoff amplitude of 75%.

Figure 3. Amplification of radar amplitudes: gain function. (**a**) The three-point manual gain function applied to all traces; (**b**) original A-scan; (**c**) A-scan after gain application.

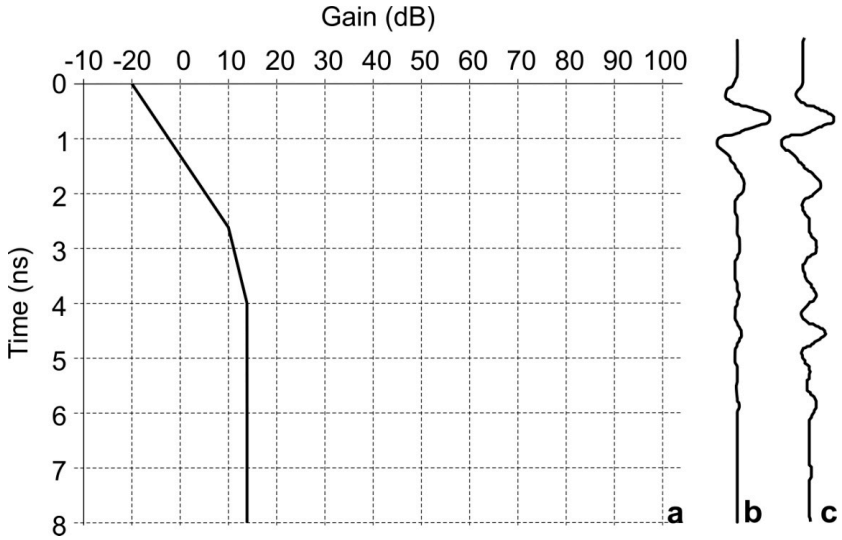

2.2. Seismic Tomography

Seismic tomography used in the evaluation of the column consisted of 2D reconstruction based on the travel-transmitted wave amplitude. Images were exclusively obtained from the first arrival of the waves, which allows the best resolution possible, as those first arrivals are always clearly detected. The first arrival offers a precision of approximately 1/10 its period. Good contact between the sensors and surface was obtained using wax to fix the accelerometers to the surface of the column. This material guarantees the proper signal transmission in the case of frequencies lower than 10 kHz and avoids damages on the structure.

Data was obtained along the 201-cm perimeter of the column. An instrumented hammer was used as the seismic source (Figure 4). Data were acquired with a high frequency sensitivity accelerometer, scanned at 63,500 samples per second. The theoretical coverage for non-refracted rays travelling from the source (hammer) to receivers (accelerometers) is showed in Figure 4. These straight trajectories can be defined by solving the equations:

$$t_i = \sum_j x_{ij}\, v_j \tag{1}$$

t_i being the travel time between source and received, measured in the survey, v_j the seismic wave velocity and x_{ij} the wave trajectory.

In order to cover the whole space, the medium is divided into cells or elements, and the results are obtained as the sum of the values in each of the cells. In the case of non-homogeneous media, the seismic wave is refracted, because of changes in the wave velocity associated with adjacent cells,

and equations are solved in an iterative computational process until convergence of the solution. The computational process, the simultaneous interactive reconstruction technique (SIRT), contemplates ray curvature as a consequence of internal refractions ([22,23]). The characteristics of each cell are defined in the case that at least one ray path crosses the cell.

Figure 4. Seismic tomography. (**a**) Position of the accelerometers around the column; (**b**) seismic survey; (**c**) ray paths in a hypothetic homogeneous column. The numbers corresponds to the position of the receivers and the source points.

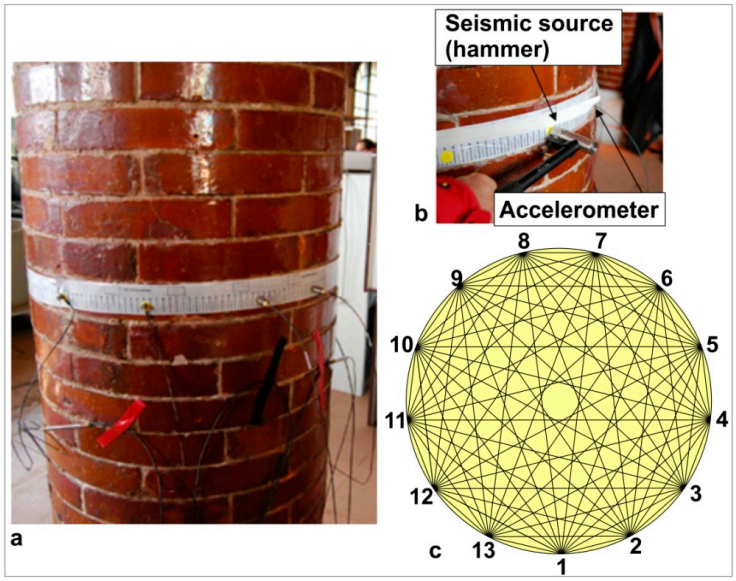

3. GPR Results

Radar data were obtained from 28 vertical profiles and 20 horizontal profiles. Radar data from vertical profiles are b-scans in Cartesian coordinates, the radar data being from the horizontal profiles' b-scan in polar coordinates. Figure 5 presents the position of the vertical radar lines on the specimen and radar data obtained in one of these profiles. The main features observed in this image correspond to two strong reflections and the irregular anomalies between them. Interpretation of the radar image is also shown in Figure 5. The shallowest strong anomaly (labelled B in Figure 5) could be due to the thickness of the external bricks. However, this anomaly is irregular, most likely as a consequence of the internal asymmetrical faces of the bricks. Its shape seems to indicate that the external bricks are not a uniform layer, although in the surface of the column, the external faces present a regular pattern (Figure 4). This hypothesis could be supported also by the non-homogeneous deeper anomalies (labelled D in Figure 5), which seem to be caused by irregular materials inside of the column. The second strong anomaly (C in Figure 5) presents a quite continuous shape and could be caused by a regular element in the central part of the column. The strong reflection probably indicates a metallic element. This anomaly is weaker or even disappear in some parts of the profile (E in Figure 5), indicating possible discontinuities. It is also remarkable that the anomaly is detected at similar depths in all of the profiles, although small time fluctuations could denote changes in the average wave propagation.

Figure 5. Distribution of the vertical radar lines on the column (**a**) and one of the radar images obtained in the profile (P) (**b**); four main detected anomalies are marked on the radar data interpretation, shown in (**c**): A: reflection on the surface of the column; B: reflection on the contact between the external bricks and other inner materials; the non-regular reflection seems to indicate that the bricks are not disposed in a uniform layer. C: Reflection on an internal element, uniform along the entire column; D: reflections on irregular targets inside of the column; E: the anomaly is weaker or even disappears in some parts of the profile.

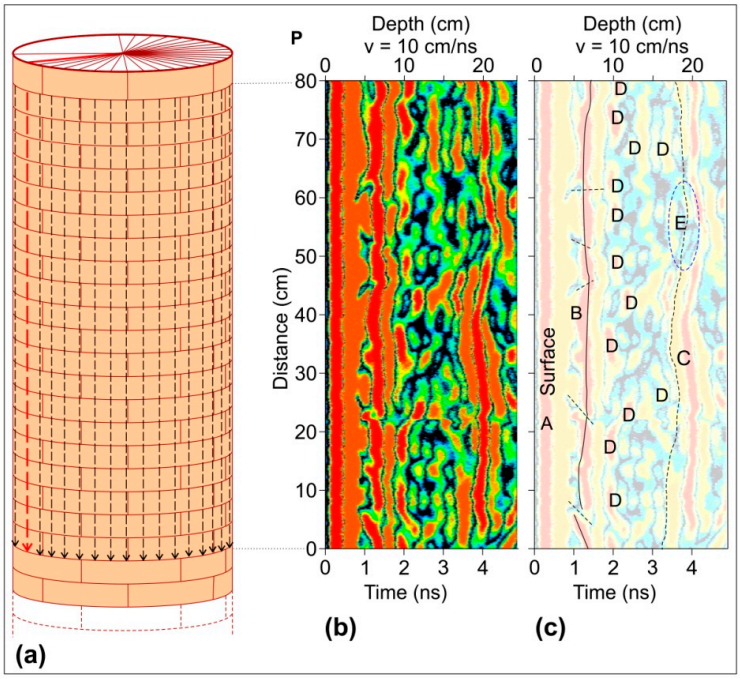

Figure 6. Radar images from six of the adjacent circular profiles.

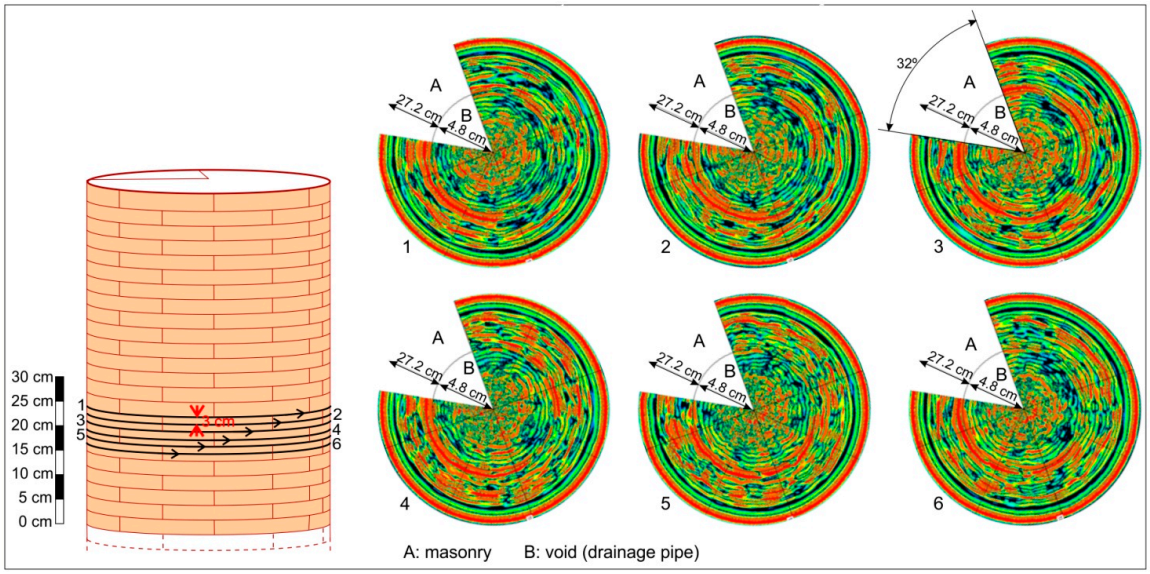

Radar data from horizontal profiles were processed in order to change from Cartesian coordinates to polar coordinates. Results were presented in circular radargrams. Those profiles were obtained in

circular radar lines, along 328°, separated 3 cm. Figure 6 presents the position of six of those horizontal radar lines on the column surface and the six radar images associated with these profiles.

Interpretation of the anomalies observed in circular profiles is shown in Figure 7. Some of the anomalies along the entire profile confirm an irregular pattern most likely associated with the internal arrangement of bricks or perhaps broken bricks. The specimen was cut after the radar exploration, and the section showed the irregular masonry arrangement.

Figure 7. Section of the column (**a**); photograph of one section; (**b**) schematic drawing, showing the different inner elements and possible interpretation of the circular profiles (1 to 6). C: anomaly caused by the internal metallic tube. D: irregular pattern as a consequence of the irregular bricks arrangement. E: the amplitude of the reflection on the tube becomes weaker in some parts.

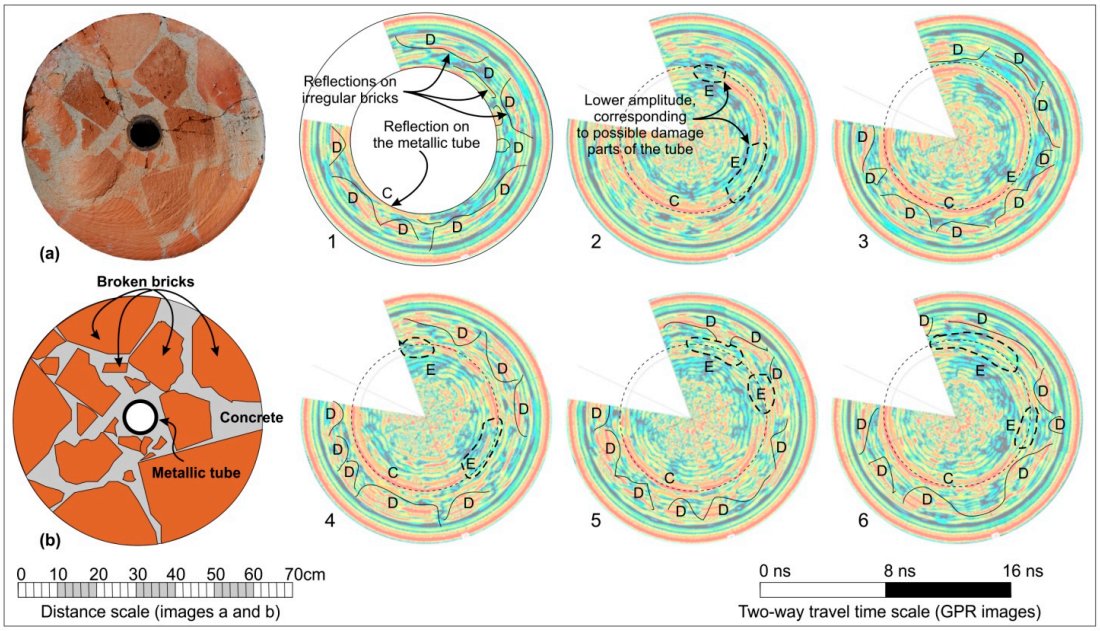

In neither circular (Figures 6 and 7) nor longitudinal (Figure 5) radar images did anomalies seem to indicate that supporting metallic structures do not exist inside the column. All anomalies are discontinuous and not strong enough to be caused by metallic targets, with the exception of the strong reflection that appears between 3.5 ns and 4 ns. This anomaly is visible in all of the circular profiles, at similar two-way travel times, indicating a possible depth of about 20 cm or 26 cm, corresponding to velocities of 10 cm/ns and 13 cm/ns. The radius of the column is 32 cm. Hence, this anomaly could be caused by the reflection on a metallic tube in the center of the column, with a diameter of about 10 cm. It is noticeable that this anomaly is strong and continuous in some parts of the column, while in other parts, the anomaly becomes weaker or even disappears. A possible interpretation is the existence of a damaged metallic rain drain pipe inside the column. This drainage pipe was later revealed when the sample was broken. Damages in this tube could explain the moisture pathologies observed in the external part of the column.

This notwithstanding, radar data are difficult to interpret as a consequence of the large number of small and irregular anomalies. Some of these elements, firstly associated with irregular bricks, could be also caused by cracks inside the column. In addition, the evaluation of the drainage pipe conditions

could be crucial to determine the possible areas where dampness may become an important pathology. Nevertheless, the extension of the pipe damage is difficult to evaluate by using only B-scans. Consequently, three-dimensional images were obtained in order to achieve a more complete visualization of the inner tube and other possible internal and important targets. 3D images were extracted by using the square of the amplitude in each A-scan and by interpolation in cylindrical coordinates. Rendered images with amplitudes higher than 75% provide proper images of the pipe (Figure 8). Results underscore the existence of the longitudinal body along the column, but evidencing the existence of some parts where the image disappears. Discontinuities are approximated to damaged parts of the pipe. Nevertheless, it is not possible to associate absolutely the discontinuities in the isoamplitude images with the parts of the tube that are completely broken, because small cracks in the pipe, voids in the masonry near the pipe or changes in the materials of the masonry column could also affect the amplitude of the wave. These amplitudes could be smaller than the 75% cut-off value considered in the rendered isoamplitude image. The use of small cut-off amplitudes did not improve the resolution in this particular case study, because of the complexity of the structure. The heterogeneous materials produce numerous reflections, obtaining confused images in the rendered isoamplitude for smaller cut-off values.

Figure 8. Three-dimensional images of the column. (**a**) Scheme of the tested specimen. One hundred meters were tested by means of circular GPR profiles. (**b**) The 3D composition of some circular radargrams. (**c**) The isosurface render generated with GPRSlice software, showing the anomaly that probably corresponds to the inner pipe and other smaller targets. (**d**) Image of the isosurface corresponding to amplitudes higher than 75% of the maximum amplitude. Changes in the amplitude could reveal the existence of possible damages corresponding to void areas in the rendered isosurface.

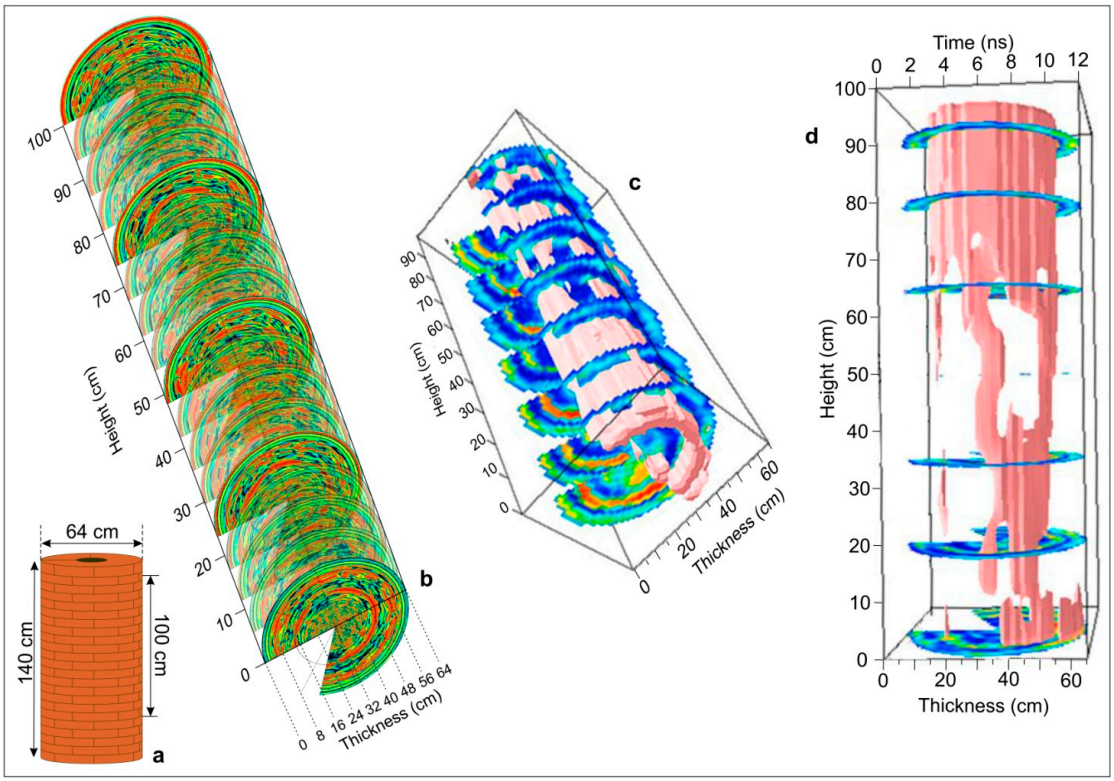

Other possible causes of the changes in the amplitude could be the corrosion of parts of the tube. The effects on the GPR signals as a consequence of the corrosion of metallic bars embedded in concrete had been proposed in 2009 by [24], and some tests were presented in 2013 by [25], concluding that bar corrosion increases the average wave velocity, the amplitude and the frequency of the bar reflection. However, in the study of the masonry column, the inhomogeneous and irregular medium impedes the possibility of detecting or identifying changes in the radar data that could be related to corrosion effects.

4. Results of Complementary Inspections

The same column was later studied with seismic tomography, endoscopy and compression tests. The results obtained with seismic and endoscopy tests were compared to radar images. Finally, the broken specimen was photographed to compare the images to the NDT results.

Seismic tomography seems to confirm the existence of the pipe in the center of the column. In this zone, a circular area presents high seismic propagation velocity (Figure 9). Several zones of the section presenting lower velocities could be associated with cracks or more damaged parts of the column. In some cases, it could be caused by the elements used in the further restoration of the column. These low-velocity zones are usually placed close to the pipe or in the shallowest part of the column. Irregular and small changes on the velocity are most likely caused by the irregular arrangement of materials inside the structure. However, it is noticeable that the column exhibits high homogeneity, with the stronger changes happening only in two small areas. The outer low-velocity area corresponds to an area of the column with visible damages. Seismic results underscore the interpretation of the GPR data. It is also remarkable that the high velocity of the inner part of the possible tube is an artifice of the software used. The low velocity of seismic waves in air caused no rays to cross this section, producing an incorrect and artificial interpolation.

Figure 9. Seismic tomography results. Changes in seismic velocity indicate the existence of different zones and irregular materials.

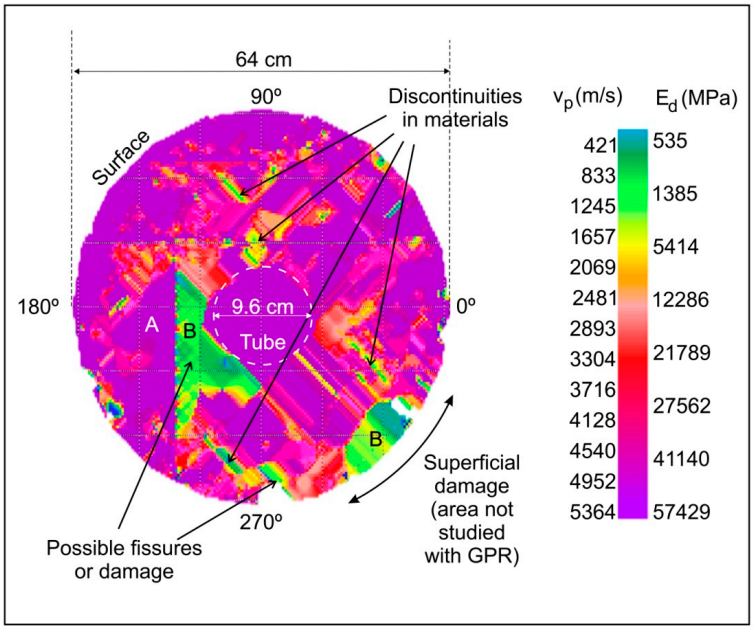

Endoscopy is a visual-inspection tool for areas inaccessible to direct eye inspection. It is a usual methodology in complex structures. Many applications combine endoscopy with non-destructive testing ([26,27]) to analyze specific images. The methodology consists of introducing a borescope in a small drilling hole (usually with a diameter less than 12 mm), to inspect the interior of the structures. The borescope is a flexible tube with a light source and an eye piece. As a result, images of the interior of the structure could provide qualitative information about changes in materials or the existence of inner voids or cracks. However, qualitative information is not achievable, because of the impossibility of inferring the real size of the elements observed in the images.

Images obtained from the interior of the column (Figure 10) confirm the existence of different materials and a damaged metallic element. In some cases, cracks appear on the images associated with bricks, highlighting some of the pathologies affecting the interior of the column.

Figure 10. Some endoscopy images, highlighting different parts and damages inside the column.

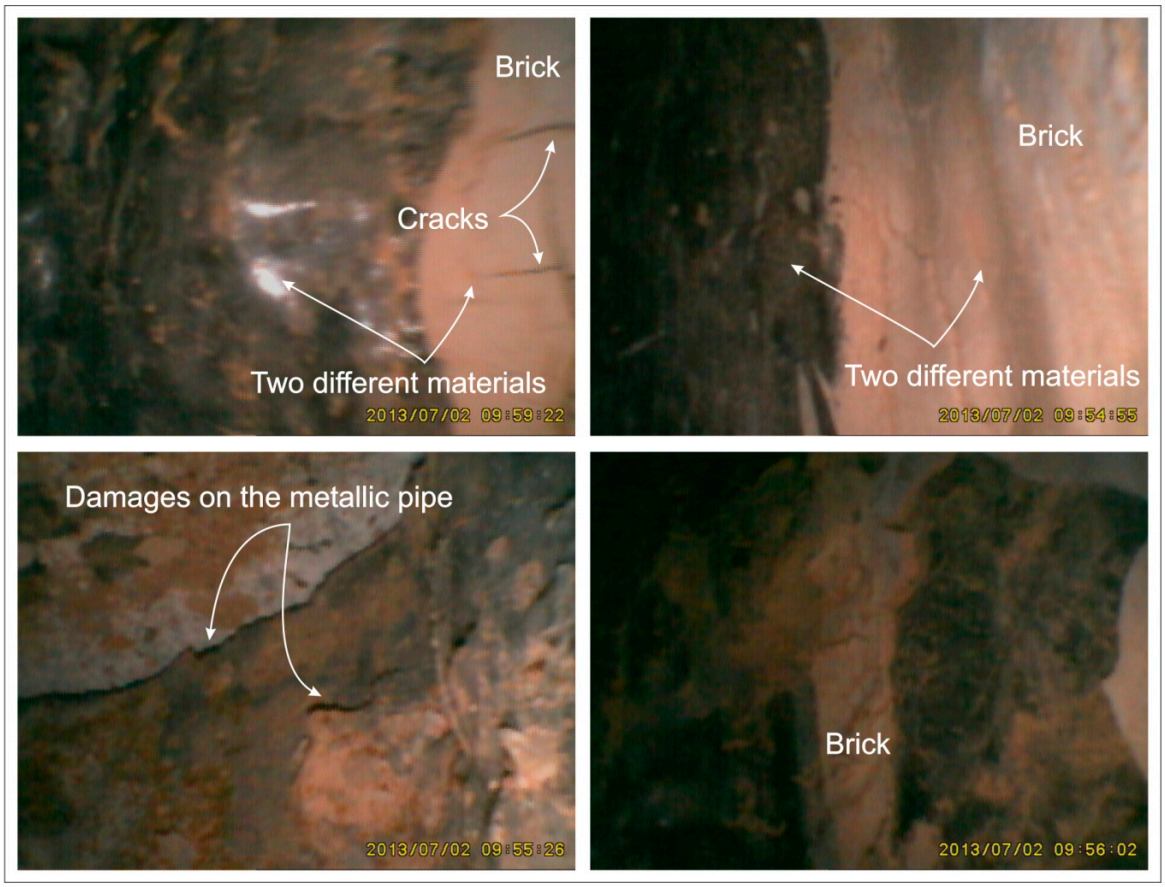

Finally, after the non-destructive surveys, a compression test was applied to the column. Hence, the column was broken, and the different elements became visible. The inner metallic pipe was extracted, and the direct visual inspection allowed for observing the damages as a consequence of corrosion. Figure 11 presents a photograph of the broken column and part of the extracted tube. This image is in concordance with the GPR and seismic images, showing the irregular arrangement of the bricks, disposed in triangular sections. The photograph of the drainage pipe section is also compared to the 3D radar render imaging, confirming the initial hypothesis about the damages.

Figure 11. (**a**) Section of the column after the compression test and (**b**) the metallic tube extracted, compared to (**c**) 3D radar imaging from isoamplitudes after a cylindrical interpolation.

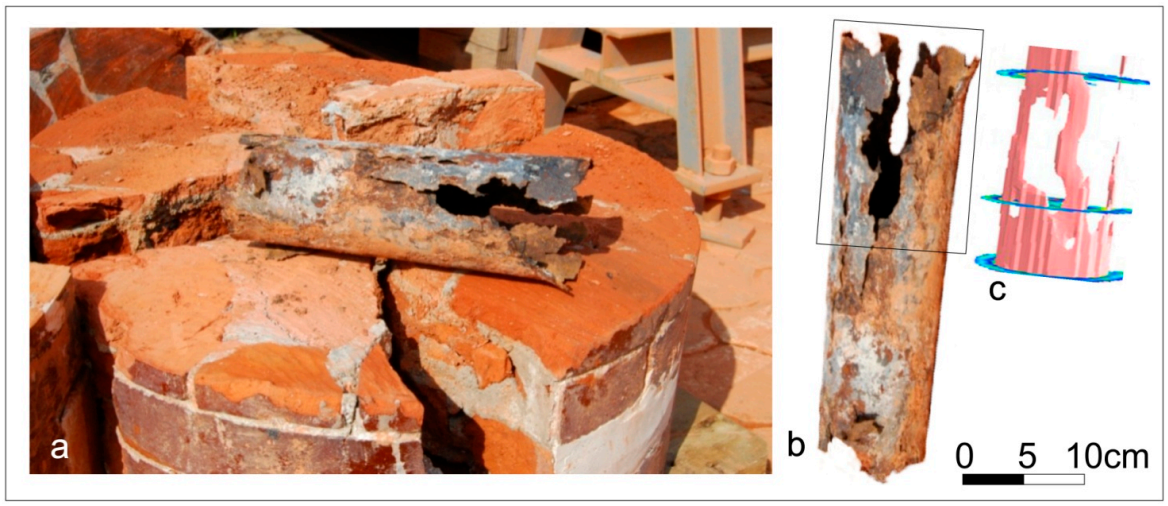

5. Discussion

The combined study of the column specimen under laboratory conditions allows defining the previous hypothesis about the structure and the pathologies affecting the member. Nuzzo and Quarta (2012) [18] describe some of the common features that could be found in cylindrical homogeneous columns and discuss the most feasible way to detect them with GPR, indicating possible open issues. Common offset mode in longitudinal profiles along the column is recommended to detect thin tubes, like vertical rebar, circular profiles being recommended in order to detect annular targets.

The evaluation of a highly irregular internal media in cylindrical columns presents additional difficulties, mainly as a consequence of complex radargrams. Radar data show asymmetrical and irregular anomalies, associated with the irregular organization of the different components. However, it was not possible to differentiate between reflections on cracks and reflections on small pieces of bricks, and the final radargrams result in complicated images. Although vertical profiles allow one to obtain radar data detecting a large number of features, circular radargrams are helpful images in the final interpretation, allowing an easier association of the anomalies to the different parts of the specimen. As a result, interpretation of the circular radar data seems to be easier than interpretation of longitudinal radargrams, in the case of small and irregular targets inside the column, presenting some kind of annular arrangement, as in the case of the asymmetrical and broken bricks. These asymmetric bricks are placed approximately in triangles. Hence, longitudinal profiles allow determining the position of anomalies, but circular profiles define, approximately, the triangular arrangement of irregular pieces.

Seismic inspection allows defining some small areas characterized by their low wave velocity, most likely related to damages. Other subtler changes could be associated with changes in materials (bricks and mortar). Like the radar images, seismic tomography presents an irregular pattern, it being difficult to associate each one of the elements with singular targets.

Radar images also underscore the absence of metallic supports, such as rebar, strengthening the column. This result must be considered in future structural analysis. In this case, longitudinal radargrams are the most appropriate to determine the existence or absence of this kind of target. This result is according to Nuzzo and Quarta [18]. This notwithstanding, radar images show the possible existence of a central metallic element, along the whole specimen. The anomaly can be distinguished in both longitudinal and circular radargrams. It is associated with a rain drainage pipe placed in the center of the column. The existence of this element was also detected in the seismic tomographic images, which present a homogeneous central area of the image without changes in velocity as a consequence of the interpolation process in the void area. Then, the non-destructive inspection indicates that, most likely, the column is entirely built with masonry, and no metallic supports are used to strengthen the structure. The only metallic target is the rain drainage tube, visible in all of the profiles in the central part. Changes in the amplitude of the reflected wave corresponding to different sections of the tube indicate possible deteriorated parts of the metallic element. A complete *in situ* inspection of a large number of selected columns of the buildings before possible structural evaluations could be recommended. The complete NDT survey would be used to detect possible changes in constructive techniques and also to define the columns with drainage pipes that could be considered potential damaged elements as a consequence of moisture.

Three-dimensional images provide useful information to understand better the most important targets inside the column, detecting the most damaged zones associated with lower amplitudes. Hence, possible damages in the central metallic tube are identified. Pathologies could be related to the corrosion of the inner drainage pipe. Humidity affects parts of the column as consequence of the tube damage, and the effects are even visible in some parts of the specimen. In other parts, dampness could be the cause of other possible internal damages. However, 3D images are not useful to evaluate small or low reflective targets inside the column. Moreover, the 3D image of the internal tube provides an accurate, but not exact, pattern of the damaged structured. Possible causes are that the received energy changes not only depend on the tube, but also on the other targets inside the column. As a result, the amplitude of the wave arriving at the central tube is not completely homogeneous, affecting the interpolation. It is also noticeable that cracks and fissures or other discontinuities under the resolution are not detected as a clear reflection, even though they could modify the amplitude of the received signal.

After the NDT inspection under laboratory conditions, the column was broken. The images from the broken column confirm the hypothesis about the interior structure, showing the irregular bricks that are arranged in, approximately, triangular shapes, differing from one another. In addition, damage in some zones was also visible in parts of the column, confirming the information from the non-destructive testing that indicates the possible existence of discontinuities or pathologies.

6. Conclusions

This paper presents the results of three laboratory tests applied to one specimen: ground penetrating radar, seismic tomography and endoscopy. The specimen is part of one masonry column extracted from a cultural heritage complex of buildings. The objective was to evaluate the information that could

be obtained with GPR and seismic surveys from these cylindrical elements. The results and conclusions will be used in future *in situ* tests, prior to the structural assessment of the buildings.

The general conclusion of this evaluation is that combined geophysical methods (GPR and seismic tomography) could successfully describe the shape of the different elements located inside the column, allowing the determination of their configuration. Combined methodologies could be useful in the study of cultural heritage structures, because GPR has demonstrated its capability to detect the arrangement of materials, allowing the definition of possible constructive methods for columns. Additionally, seismic tomography and endoscopy provide helpful images to compare to radar data, preventing possible uncertainties.

The results show other particular, but interesting, conclusions related to the evaluation of cylindrical masonry elements:

(1) GPR inspection of cylindrical columns could be executed with longitudinal profiles along the column or with perimetric profiles around the column. In the first case, radar data provide useful information about longitudinal targets that appear along the whole record. Hence, the results are useful to detect possible reinforcement bars or changes in materials affecting the same depth of the whole structure. These profiles were, in the study described in this paper, greatly valuable to refuse a previous hypothesis about the constructive structure, demonstrating the absence of rebar or other reinforcing elements in the column. However, it was not possible to determine the masonry arrangement with data from vertical profiles.

(2) Perimetric profiles must be converted into polar coordinates for proper interpretation of the results. In the radar data obtained with these profiles, images allow one to define the arrangement of the materials inside the column. The irregular bricks and groups of bricks identified in these radargrams result in confusing anomalies in the vertical profiles. It should be noted that the spacing between profiles must be adequate to detect the abrupt changes in materials. Hence, the dimensions of the external faces of the bricks determine the separation between perimetric profiles.

(3) Differentiating between voids or cracks and changes in materials is difficult only with GPR data. Combined interpretation of seismic and GPR data defines the possible target better, because changes in seismic velocities highlight the existence of damaged areas. Endoscopy is also particularly useful because it provides images of the targets that could be associated with the different radar or seismic anomalies.

(4) The results demonstrate the existence of a longitudinal metallic target. This element was clearly visible in seismic tomography and in both perimetric and longitudinal GPR profiles. The inspection of the different parts of the column after the analysis demonstrates that the anomaly detected during the non-destructive testing was caused by a rainwater drainage pipe.

(5) The metallic pipe was deteriorated because of corrosion. This damage is not detected in the seismic tomography, but perimetric radar images reveal the existence of zones with important decreases in the reflected wave amplitude. Three-dimensional volumes were defined by interpolating all radar profiles. These images properly define the metallic tube and also the areas most affected by damage.

(6) The GPR 3D render images do not define exactly the shape of the breakage due to the corrosion. Two main causes could be pointed out to explain this fact. The first one is that the column is built with many irregular elements that cause reflections and the diffraction of the energy differently from point to point. Hence, the amplitude of the wave that arrives at the tube is not always the same. This fact is also highlighted because of the differences in the two-way travel of the energy reflected on the surface of the pipe, which is recorded between 3 ns and 4 ns, revealing changes in the average wave velocity. The second one is a consequence of the interpolation of profiles.

The results obtained in this study must be considered in future structural evaluation. It is recommended to evaluate a large number of columns before the evaluation, in order to assure that the constructive methodology is the same in all of the elements. On the other hand, it is also recommended to detect the columns with drainage pipes, to define the elements that could be affected by pathologies caused by dampness in the future. The methodology proposed in this laboratory evaluation could be used to obtain enough information in preventive forthcoming evaluations.

Acknowledgments

This work has been partially funded by the Spanish Government and by the European Commission with FEDER funds, through the research project, CGL2011-23621, and by the project "New Integrated Knowledge-based approaches to the protection of cultural heritage from Earthquake-induced Risk (NIKER)" funded by the European Commission (Grant Agreement No. 244123). The study is also a contribution to the EU-funded COST Action TU1208, "Civil Engineering Applications of Ground Penetrating Radar".

Author Contributions

Vega Perez-Gracia and Sonia Santos-Assunçao conceived, designed and performed the experiments with GPR; Oriol Caselles, Jaume Clapes and Victor Salinas conceived, designed and performed the seismic assessment and endoscopy inspection; Vega Perez-Gracia and Sonia Santos-Assunçao. analyzed the data; Sonia Santos-Assunçao constructed the 3D radar images; Vega Perez-Gracia wrote the paper.

Conflicts of Interest

The authors declare no conflict of interest.

References

1. Binda, L.; Saisi, A.; Tiraboschi, C. Investigation procedures for the diagnosis of historic masonries. *Constr. Build. Mater.* **2000**, *14*, 199–233.
2. Pérez-Gracia, V.; Canas, J.A.; Pujades, L.G.; Clapés, J.; Caselles, O.; García, F.; Osorio, R. GPR survey to confirm the location of ancient structures under the Valencian Cathedral, Spain. *J. Appl. Geophys.* **2000**, *43*, 167–174.

3. Cardarelli, E.; di Nardis, R. Seismic refraction, isotropic and anisotropic tomography on an ancient monument (Antonio and Faustina Temple AD 141). *Geophys. Prospect.* **2001**, *49*, 228–240.
4. Leucci, G.; Persico, R.; Soldovieri, F. Detection of fractures from GPR data: The case history of the Cathedral of Otranto. *J. Geophys. Eng.* **2007**, *4*, 452–461.
5. Masini, N.; Persico, R.; Guida, A.; Pagliuca, A. A multifrequency and multisensor approach for the study and the restoration of monuments: The case of the Cathedral of Matera. *Adv. Geosci.* **2008**, *19*, 17–22.
6. Pérez-Gracia, V.; García, F.; Pujades, L.G.; González-Drigo, R.; di Capua, D. GPR survey to study the restoration of a Roman monument. *J. Cult. Herit.* **2008**, *9*, 89–96.
7. González-Drigo, R.; Pérez-Gracia, V.; di Capua, D.; Pujades, L.G. GPR survey applied to Modernista buildings in Barcelona: The cultural heritage of the College of Industrial Engineering. *J. Cult. Herit.* **2008**, *9*, 196–202.
8. Hemeda, S. Ground Penetrating Radar (GPR) investigations for architectural heritage preservation: The case of Habib Sakakini Palace, Cairo, Egypt. *Open J. Geol.* **2012**, *2*, 189–197.
9. Pérez-Gracia, V.; González-Drigo, R.; di Capua, D. Horizontal resolution in a non-destructive shallow GPR survey: An experimental evaluation. *NDT&E Int.* **2008**, *41*, 611–620.
10. Rial, F.I.; Pereira, M.; Lorenzo, H.; Arias, P. Novo A. Resolution of GPR bowtie antennas: An experimental approach. *J. Appl. Geophys.* **2009**, *67*, 367–373.
11. Pérez-Gracia, V.; Caselles, J.O.; Clapés, J.; Martinez, G.; Osorio, R. Non-destructive analysis in cultural heritage buildings: Evaluating the Mallorca Cathedral supporting structures. *NDT&E Int.* **2013**, *59*, 40–47.
12. Hamrouche, R.; Klysz, G.; Balayssac, J.-P.; Rhazi, J.; Ballivy, G. Numerical simulations and laboratory tests to explore the potential of Ground-Penetrating Radar (GPR) in detecting unfilled joints in brick masonry structures. *Int. J. Architect. Herit.* **2012**, *6*, 648–664.
13. Topczewski, L.; Fernandes, F.M.; Cruz, P.J.S.; Lourenço, P.B. Practical implications of GPR investigation using 3D data reconstruction and transmission tomography. *J. Build. Apprais.* **2007**, *3*, 59–76.
14. Diamanti, N.; Giannopoulos, A.; Forde, C. Numerical modeling and experimental verification of GPR to investigate ring separation in brick masonry arch bridges. *NDT&E Int.* **2008**, *41*, 354–363.
15. Pérez-Gracia, V.; González-Drigo, R.; Sala, R. Ground-penetrating radar resolution in cultural heritage applications. *Near Surf. Geophys.* **2012**, *10*, 77–87.
16. Solla, M.; Caamaño, J.C.; Riveiro, B.; Arias, P. A novel methodology for the structural assessment of stone arches based on geometric data by integration of photogrammetry and ground-penetrating radar. *Eng. Struct.* **2012**, *35*, 96–306.
17. Ranalli, D.D.; Scozzafava, M.; Tallini, M. Ground penetrating radar investigations for the restoration of historic buildings: The case study of the Collemaggio Basilica (L'Aquila, Italy). *J. Cult. Herit.* **2004**, *5*, 91–99.
18. Nuzzo, L.; Quarta, T. GPR prospecting of cylindrical structures in cultural heritage applications: A review of geometric issues. *Near Surf. Geophys.* **2012**, *10*, 17–34.

19. Masini, N.; Persico, R.; Rizzo, E.; Calia, A.; Giannotta, M.T.; Quarta, G.; Pagliuca, A. Integrated techniques for analysis and monitoring of historical monuments: The case of San Giovanni al Sepolcro in Brindisi, southern Italy. *Near Surf. Geophys.* **2010**, *8*, 423–432.
20. Goodman, D. *GPR-SLICE. Ground Penetrating Radar Imaging Software*; User's Manual Geophysical Archaeometry Laboratory: Woodland Hills, CA, USA, 2004.
21. Goodman, D.; Piro, S.; Nishimura, Y.; Schneider, K.; Hongo, H.; Higashi, N.; Steinberg, J.; Damiata, B. GPR-SLICE GPR archaeometry. In *Ground Penetrating Radar Theory and Applications*; Jol, H.M., Ed.; Elsevier: Amsterdam, The Netherlands, 2008; pp. 479–508.
22. Michelena, R.J.; Muir, F.; Harris, J.M. Anisotropic travel time tomography. *Geophys. Prospect.* **1993**, *41*, 381–412.
23. Sandmeier, K.J. *REFLEX Program for Prospecting and Interpretation of Reflection and Transmission Data*; Karlsruhe: Sandmeier, Germany, 2003.
24. Ferrieres, X.; Klysz, G.; Mazet, P.; Balayssac, J.P. Evaluation of the concrete electromagnetics properties by using radar measurements in a context of building sustainability. *Comput. Phys. Commun.* **2009**, *180*, 1277–1281.
25. Lai, W.L.; Kind, T.; Stoppel, M.; Wiggenhauser, H. Measurement of accelerated steel corrosion in concrete using ground-penetrating radar and a modified half-cell potential method. *J. Infrastruct. Syst.* **2013**, *19*, 205–220.
26. Spagnolo, G.S.; Ambrosini, D.; Paoletti, D. An NDT electro-optic system for mosaics investigations. *J. Cult. Herit.* **2003**, *4*, 369–376.
27. Faella, G.; Frunzio, G.; Guadagnuolo, M.; Donadio, A.; Ferri, L. The church of the nativity in Bethlehem: Non-destructive tests for the structural knowledge. *J. Cult. Herit.* **2012**, *13*, 27–41.